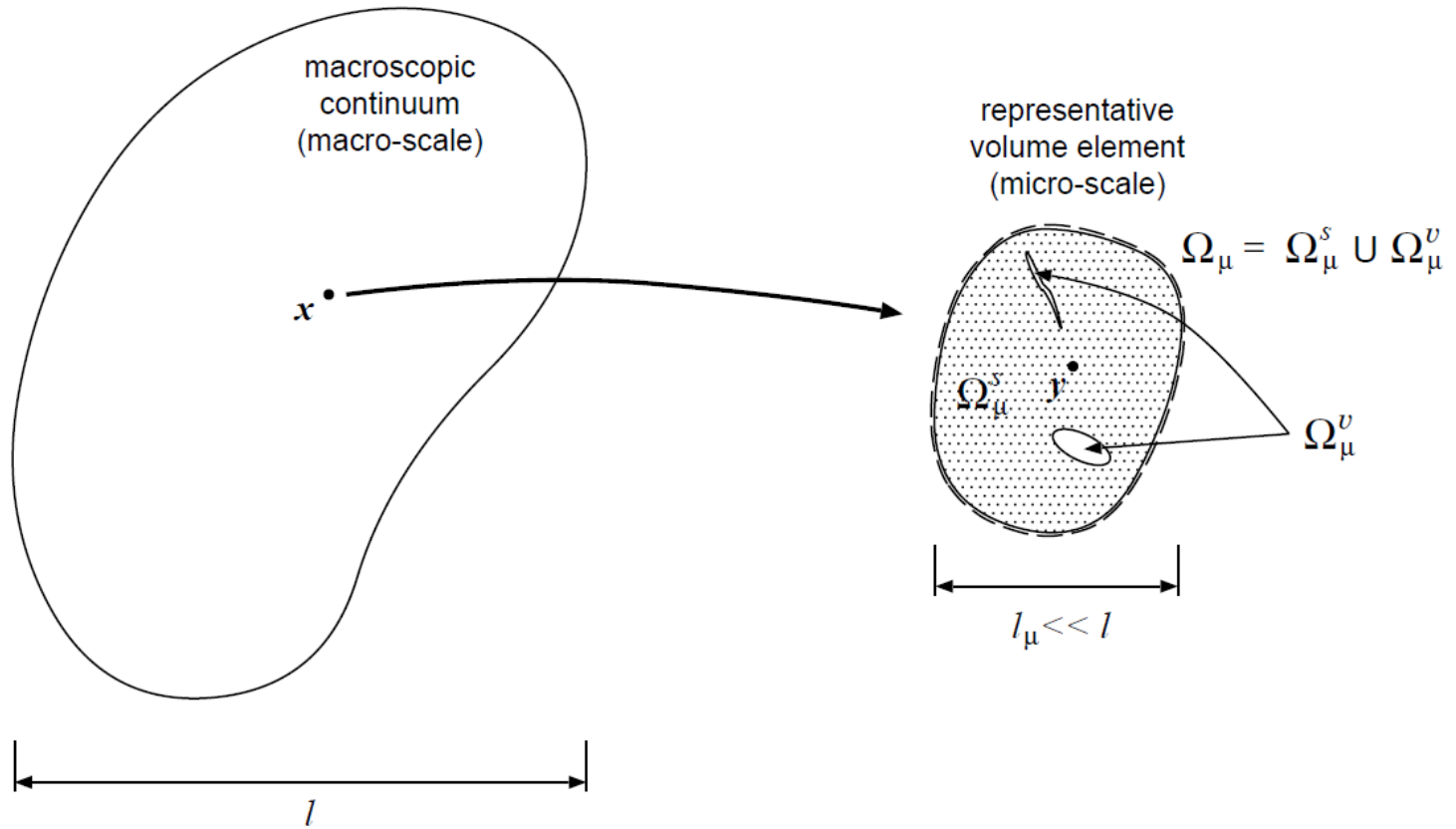


Multiscale Constitutive Modelling of Solids

Topics:

- *Multiscale constitutive theory*
- *Finite element implementation*
- *Applications*



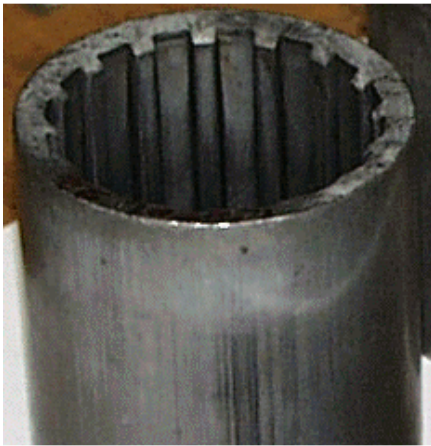
Macro-continuum and the RVE

Multiscale constitutive theory Background

- Continuum formulation
 - ◆ Foundations established by Hill (1960s) and Mandel (1971)
 - ◆ Significant contributions, especially related to mathematical concepts, by Sanchez-Palencia and Suquet (1980s)
 - ◆ Large number of works related to the estimates of material properties of heterogeneous composites (Nemat-Nasser, Hori, Willis, Ponte-Castaneda and others); still ongoing
- Computational strategies based on FE
 - ◆ Feyel and Chaboche (2000): on basic FE methodology
 - ◆ Miehe and co-workers (1999,2002,2003): on generic formulation for linear and nonlinear problems
 - ◆ Kouznetsova, Brekelmans, Baaijens, Geers (2001,2002): on basic methodology and gradient enhanced models
 - ◆ Terada and Kikuchi (2001): generic formulation for linear and nonl. pr.
 - ◆ Ladeveze and co-workers (2001): on generic strategies for composites
 - ◆ Wriggers and Zohdi (2004): computational estimates of material properties; Wriggers (2007) on homogenisation of particulate materials
 - ◆ Ibrahimbegovic and co-workers (2004)
 - ◆ Ramm and co-workers (2005): localised failure analysis
 - ◆ Belytschko et al. (2007): failure at micro-level; aggregation discontinuities

Why multiscale constitutive models ?

real workpiece



Underlying model:

Lemaitre's ductile damage
model with tensile/
compressive
damage growth distinction

Why multiscale constitutive models ?

- Improve predictive capability in numerical simulations
 - Coupled multiscale FE analysis (FE²)
 - Calibration of phenomenological (macroscopic) models
 - Devising new macroscopic models
- Understanding microscopic mechanisms and their impact on macroscopic behaviour
- Design of new materials

Multiscale Constitutive Theory

Classical internal variable-based constitutive theory

$$\boldsymbol{\sigma}(t) = \tilde{\mathfrak{F}}(\boldsymbol{\varepsilon}^t)$$

Simplest model (linear elasticity – non-dissipative)

$$\boldsymbol{\sigma}(t) = \mathbf{D}^e : \boldsymbol{\varepsilon}(t)$$

A simple dissipative model (Norton's creep law)

$$\begin{cases} \boldsymbol{\sigma} = \mathbf{D}^e : (\boldsymbol{\varepsilon} - \boldsymbol{\varepsilon}^p) \\ \dot{\boldsymbol{\varepsilon}}^p = \left(\frac{\|\text{dev } \boldsymbol{\sigma}\|}{\lambda} \right)^N \text{dev } \boldsymbol{\sigma} \end{cases}$$

$$\longrightarrow \dot{\boldsymbol{\sigma}}(t) = \mathbf{D}^e : \left[\dot{\boldsymbol{\varepsilon}}(t) - \left(\frac{\|\text{dev } \boldsymbol{\sigma}(t)\|}{\lambda} \right)^N \text{dev } \boldsymbol{\sigma}(t) \right]$$

Multiscale constitutive theory

$$\sigma(t) = \tilde{\mathfrak{F}}(\varepsilon^t)$$

... history dependence concept same as in classical theory, BUT

**The evolution of the stress is generally described by an
initial boundary value problem
at the so-called microscopic (RVE) level !!
(as opposed to ODEs in the classical case)**

Multiscale constitutive theory

Basic axioms (EA de Souza Neto & RA Feijoo, 2010)

- (i) Strain/deformation gradient averaging;
- (ii) Functional set of admissible fluctuations is a subspace of the minimally constrained space of displacement fields compatible with the deformation gradient averaging;
- (iii) Equilibrium of the RVE (principle of virtual work);
- (iv) Stress averaging; and
- (v) Hill-Mandel Principle of Macro-homogeneity.

(i) Strain averaging

$$\boldsymbol{\varepsilon}(\boldsymbol{x}, t) = \frac{1}{V_\mu} \int_{\Omega_\mu} \boldsymbol{\varepsilon}_\mu(\boldsymbol{y}, t) \, dV \quad \boldsymbol{\varepsilon}_\mu \equiv \nabla^s \boldsymbol{u}_\mu$$

Consequence Minimally constrained set of RVE displacements fields

$$\boldsymbol{u}_\mu \in \mathcal{K}_\mu^* \equiv \left\{ \boldsymbol{v}, \text{ sufficiently regular} \mid \int_{\partial\Omega_\mu} \boldsymbol{v} \otimes_s \boldsymbol{n} \, dA = V_\mu \boldsymbol{\varepsilon} \right\}$$

In terms of displacements fluctuations,

$$\begin{aligned} \tilde{\boldsymbol{u}}_\mu(\boldsymbol{y}, t) &\equiv \boldsymbol{u}_\mu(\boldsymbol{y}, t) - \{\boldsymbol{u}(\boldsymbol{x}, t) + \boldsymbol{\varepsilon} \boldsymbol{y}\} \\ \tilde{\boldsymbol{u}}_\mu \in \tilde{\mathcal{K}}_\mu^* &\equiv \left\{ \boldsymbol{v}, \text{ sufficiently regular} \mid \int_{\partial\Omega_\mu} \boldsymbol{v} \otimes_s \boldsymbol{n} \, dA = \mathbf{0} \right\} \end{aligned}$$

(ii) The actual kinematical constraints are such that

$$\tilde{\mathcal{K}}_\mu \subset \tilde{\mathcal{K}}_\mu^*$$

is a *subspace* of $\tilde{\mathcal{K}}_\mu^*$

Consequence Space of virtual displacements coincides with the space of admissible fluctuations

$$\mathcal{V}_\mu = \tilde{\mathcal{K}}_\mu$$

(iii) Equilibrium of the RVE

$$\int_{\Omega_\mu} \sigma_\mu(\mathbf{y}, t) : \nabla^s \eta \, dV - \int_{\Omega_\mu} \mathbf{b}(\mathbf{y}, t) \cdot \eta \, dV - \int_{\partial\Omega_\mu} \mathbf{t}^e(\mathbf{y}, t) \cdot \eta \, dA = 0 \quad \forall \eta \in \mathcal{V}_\mu$$

(iv) Stress averaging

$$\sigma(\mathbf{x}, t) \equiv \frac{1}{V_\mu} \int_{\Omega_\mu} \sigma_\mu(\mathbf{y}, t) \, dV$$

(v) Hill-Mandel Principle

$$\sigma : \dot{\epsilon} = \frac{1}{V_\mu} \int_{\Omega_\mu} \sigma_\mu : \dot{\epsilon}_\mu \, dV$$

Consequences

- **Body force and external traction fields are orthogonal to \mathcal{V}_μ (reactive load systems to the chosen kinematical constraints)**

$$\int_{\partial\Omega_\mu} \mathbf{t}^e \cdot \boldsymbol{\eta} \, dA = 0; \quad \int_{\Omega_\mu^s} \mathbf{b} \cdot \boldsymbol{\eta} \, dV = 0 \quad \forall \boldsymbol{\eta} \in \mathcal{V}_\mu$$

- Reduced RVE equilibrium problem

$$G(\boldsymbol{\varepsilon}, \tilde{\mathbf{u}}_\mu, \boldsymbol{\eta}) \equiv \int_{\Omega_\mu^s} \mathfrak{F}_y \{ [\boldsymbol{\varepsilon}(\mathbf{x}, t) + \nabla^s \tilde{\mathbf{u}}_\mu(\mathbf{y}, t)]^t \} : \nabla^s \boldsymbol{\eta} \, dV$$

$$- \int_{\partial\Omega_\mu^v} \mathbf{t}^v(\mathbf{y}, t) \cdot \boldsymbol{\eta} \, dA = 0 \quad \forall \boldsymbol{\eta} \in \mathcal{V}_\mu$$

where it is generally assumed that $\boldsymbol{\sigma}_\mu(\mathbf{y}, t) = \mathfrak{F}_y(\boldsymbol{\varepsilon}_\mu^t(\mathbf{y}))$

The choices of \mathcal{V}_μ

(a) Taylor model

$$\mathcal{V}_\mu = {}^{\text{Taylor}}\mathcal{V}_\mu \equiv \{\mathbf{0}\}$$

(b) Linear boundary displacements model

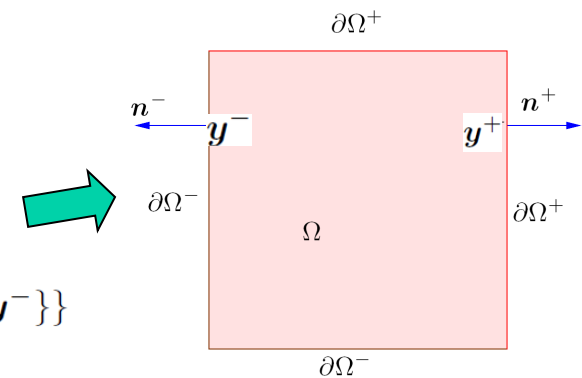
$$\mathcal{V}_\mu = {}^{\text{lin}}\mathcal{V}_\mu \equiv \{ \tilde{\mathbf{u}}_\mu \in \tilde{\mathcal{K}}_\mu^* \mid \tilde{\mathbf{u}}_\mu(\mathbf{y}, t) = \mathbf{0} \quad \forall \mathbf{y} \in \partial\Omega_\mu \}$$

(c) Periodic boundary displacements fluctuations model

$$\begin{aligned} \mathcal{V}_\mu &= {}^{\text{per}}\mathcal{V}_\mu \\ &\equiv \{ \tilde{\mathbf{u}}_\mu \in \tilde{\mathcal{K}}_\mu^* \mid \tilde{\mathbf{u}}_\mu(\mathbf{y}^+, t) = \tilde{\mathbf{u}}_\mu(\mathbf{y}^-, t) \quad \forall \text{ pairs } \{\mathbf{y}^+, \mathbf{y}^-\} \} \end{aligned}$$

(d) Minimum kinematical constraint (or uniform boundary traction)

$$\mathcal{V}_\mu \equiv \left\{ \mathbf{v}, \text{ sufficiently regular} \mid \int_{\partial\Omega_\mu} \mathbf{v} \otimes_s \mathbf{n} \, dA = \mathbf{0} \right\}$$



Remarks

- Note that

$$\text{Taylor}_{\mathcal{V}_\mu} \subset \text{lin}_{\mathcal{V}_\mu} \subset \text{per}_{\mathcal{V}_\mu} \subset \text{uni}_{\mathcal{V}_\mu}$$

That is, the Taylor model results in **stiffest** response (**upper bound**), while uniform traction results in the **softest** response (**lower bound**).

- The use of different \mathcal{V}_μ for a given RVE generally produces **different estimates**.
- The choice of \mathcal{V}_μ (the **kinematical constraints**) for a given RVE fully **defines the model** !

The macroscopic constitutive tangent tensor

$$\mathbb{C} = \bar{\mathbb{C}} + \tilde{\mathbb{C}}$$


where $\bar{\mathbb{C}}$ is the Taylor (volume average) constitutive tangent tensor and

$$\tilde{\mathbb{C}} = \left[\frac{1}{V_\mu} \int_{\Omega_\mu} (\tilde{\mathbf{T}}_{\mu kl})_{ij} \right] (\mathbf{e}_i \otimes \mathbf{e}_j \otimes \mathbf{e}_k \otimes \mathbf{e}_l) \quad \tilde{\mathbf{T}}_{\mu ij} = \mathbb{C}_\mu \nabla^s \tilde{\mathbf{u}}_{\mu ij}$$

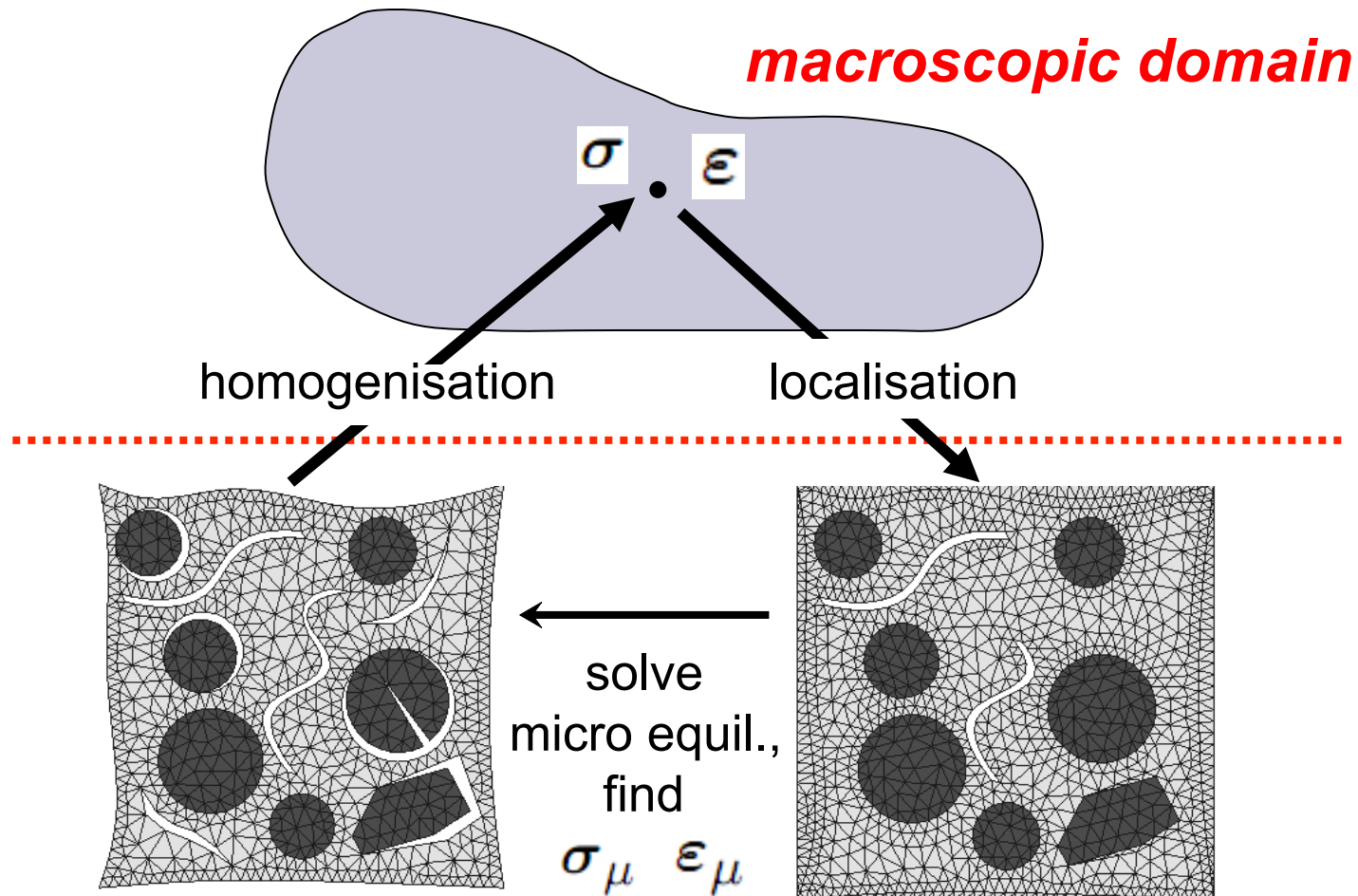
$$\int_{\Omega_\mu} \mathbb{C}_\mu \nabla^s \tilde{\mathbf{u}}_{\mu ij} \cdot \nabla^s \boldsymbol{\eta} = - \int_{\Omega_\mu} \mathbb{C}_\mu (\mathbf{e}_i \otimes \mathbf{e}_j) \cdot \nabla^s \boldsymbol{\eta} \quad \forall \boldsymbol{\eta} \in \mathcal{V}_\mu$$

Multiscale constitutive theory

Typical applications

- Coupled multiscale FE analysis (FE^2)  expensive!
- Calibration of phenomenological (macroscopic) models
- Devising new macroscopic models
- Understanding microscopic mechanisms and their impact on macroscopic behaviour
- Design/optimisation of microstructures

Application. Fully coupled FE analysis



discretised macroscopic domain (RVE)

Finite element solution of the RVE equil. problem

Discretised RVE non-linear equilibrium problem

$$G^h(\tilde{\mathbf{u}}_\mu^{n+1}) \equiv \left\{ \int_{\Omega_\mu^h} \mathbf{B}^T \hat{\boldsymbol{\sigma}}_y(\boldsymbol{\varepsilon}^{n+1} + \mathbf{B} \tilde{\mathbf{u}}_\mu^{n+1}) \, dV \right\} \cdot \boldsymbol{\eta} = 0$$

$$\forall \boldsymbol{\eta} \in \tilde{\mathcal{K}}_\mu^h$$

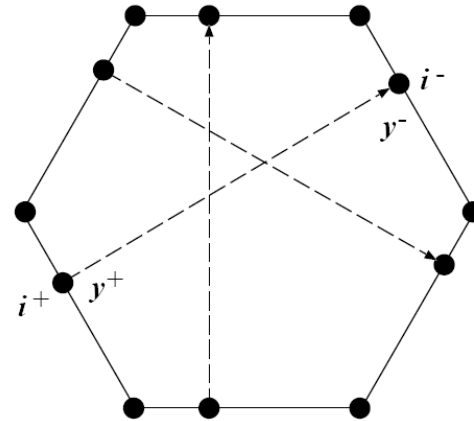
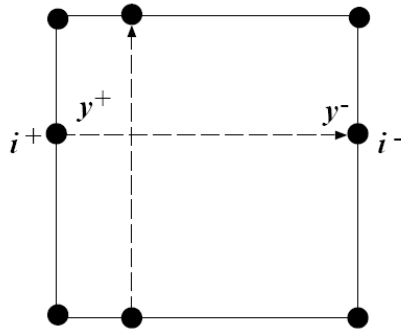
Linearised form. Newton-Raphson iteration

$$\left[\mathbf{F}^{(k-1)} + \mathbf{K}^{(k-1)} \delta \tilde{\mathbf{u}}_\mu^{(k)} \right] \cdot \boldsymbol{\eta} = 0 \quad \forall \boldsymbol{\eta} \in \tilde{\mathcal{K}}_\mu^h$$

$$\mathbf{F}^{(k-1)} \equiv \int_{\Omega_\mu^h} \mathbf{B}^T \hat{\boldsymbol{\sigma}}_y(\boldsymbol{\varepsilon}^{n+1} + \mathbf{B} \tilde{\mathbf{u}}_\mu^{(k-1)}) \, dV,$$

$$\mathbf{K}^{(k-1)} \equiv \int_{\Omega_\mu^h} \mathbf{B}^T \mathbf{D}^{(k-1)} \mathbf{B} \, dV$$

Periodic boundary fluctuations



$$\tilde{\mathcal{K}}_{\mu}^h = \left\{ \mathbf{v} = \begin{bmatrix} \mathbf{v}_i \\ \mathbf{v}_+ \\ \mathbf{v}_- \end{bmatrix} \mid \mathbf{v}_+ = \mathbf{v}_- \right\}$$

$$\longrightarrow \left\{ \begin{bmatrix} \mathbf{F}_i \\ \mathbf{F}_+ \\ \mathbf{F}_- \end{bmatrix}^{(k-1)} + \begin{bmatrix} \mathbf{k}_{ii} & \mathbf{k}_{i+} & \mathbf{k}_{i-} \\ \mathbf{k}_{+i} & \mathbf{k}_{++} & \mathbf{k}_{+-} \\ \mathbf{k}_{-i} & \mathbf{k}_{-+} & \mathbf{k}_{--} \end{bmatrix}^{(k-1)} \begin{bmatrix} \delta \tilde{\mathbf{u}}_i \\ \delta \tilde{\mathbf{u}}_+ \\ \delta \tilde{\mathbf{u}}_+ \end{bmatrix}^{(k)} \right\} \cdot \begin{bmatrix} \boldsymbol{\eta}_i \\ \boldsymbol{\eta}_+ \\ \boldsymbol{\eta}_+ \end{bmatrix} = 0 \quad \forall \boldsymbol{\eta}_i, \boldsymbol{\eta}_+$$

Minimum constraint (uniform traction)

$$\tilde{\mathcal{K}}_{\mu}^h \equiv \left\{ \mathbf{v} = \begin{bmatrix} \mathbf{v}_i \\ \mathbf{v}_b \end{bmatrix} \mid \int_{\partial\Omega_{\mu}^h} \mathbf{N}_b \mathbf{v}_b \otimes_s \mathbf{n} \, dA = \mathbf{0} \right\}$$

$\mathbf{C} \mathbf{v}_b = \mathbf{0}$

Global constraint matrix

$$\mathbf{C} = \begin{bmatrix} \int_{\partial\Omega_{\mu}^h} N_{k+1} n_1 \, dA & 0 & \cdots & \int_{\partial\Omega_{\mu}^h} N_{k+m} n_1 \, dA & 0 \\ 0 & \int_{\partial\Omega_{\mu}^h} N_{k+1} n_2 \, dA & \cdots & 0 & \int_{\partial\Omega_{\mu}^h} N_{k+m} n_2 \, dA \\ \int_{\partial\Omega_{\mu}^h} N_{k+1} n_2 \, dA & \int_{\partial\Omega_{\mu}^h} N_{k+1} n_1 \, dA & \cdots & \int_{\partial\Omega_{\mu}^h} N_m n_2 \, dA & \int_{\partial\Omega_{\mu}^h} N_m n_1 \, dA \end{bmatrix}$$

Elemental constraint matrix (for an 8-noded isoparametric quad)

$$\mathbf{C}^{(e)} = l^{(e)} \begin{bmatrix} \frac{1}{6} & 0 & \frac{2}{3} & 0 & \frac{1}{6} & 0 \\ 0 & 0 & 0 & 0 & 0 & 0 \\ 0 & \frac{1}{6} & 0 & \frac{2}{3} & 0 & \frac{1}{6} \end{bmatrix}$$

$$\begin{bmatrix} \mathbf{C}_f & \mathbf{C}_d & \mathbf{C}_p \end{bmatrix} \begin{bmatrix} \mathbf{v}_f \\ \mathbf{v}_d \\ \mathbf{v}_p \end{bmatrix} = \mathbf{0} \quad \mathbf{v}_p = \mathbf{0}; \text{ (no rigid body motion)}$$

$$\longrightarrow \begin{bmatrix} \mathbf{C}_f & \mathbf{C}_d \end{bmatrix} \begin{bmatrix} \mathbf{v}_f \\ \mathbf{v}_d \end{bmatrix} = \mathbf{0}$$

$$\longrightarrow \mathbf{v}_d = \mathbf{R} \mathbf{v}_f \quad \mathbf{R} \equiv -\mathbf{C}_d^{-1} \mathbf{C}_f$$

$$\longrightarrow \tilde{\mathcal{H}}_\mu^h \equiv \left\{ \mathbf{v} = \begin{bmatrix} \mathbf{v}_i \\ \mathbf{v}_f \\ \mathbf{v}_d \end{bmatrix} \mid \mathbf{v}_d = \mathbf{R} \mathbf{v}_f \right\}$$

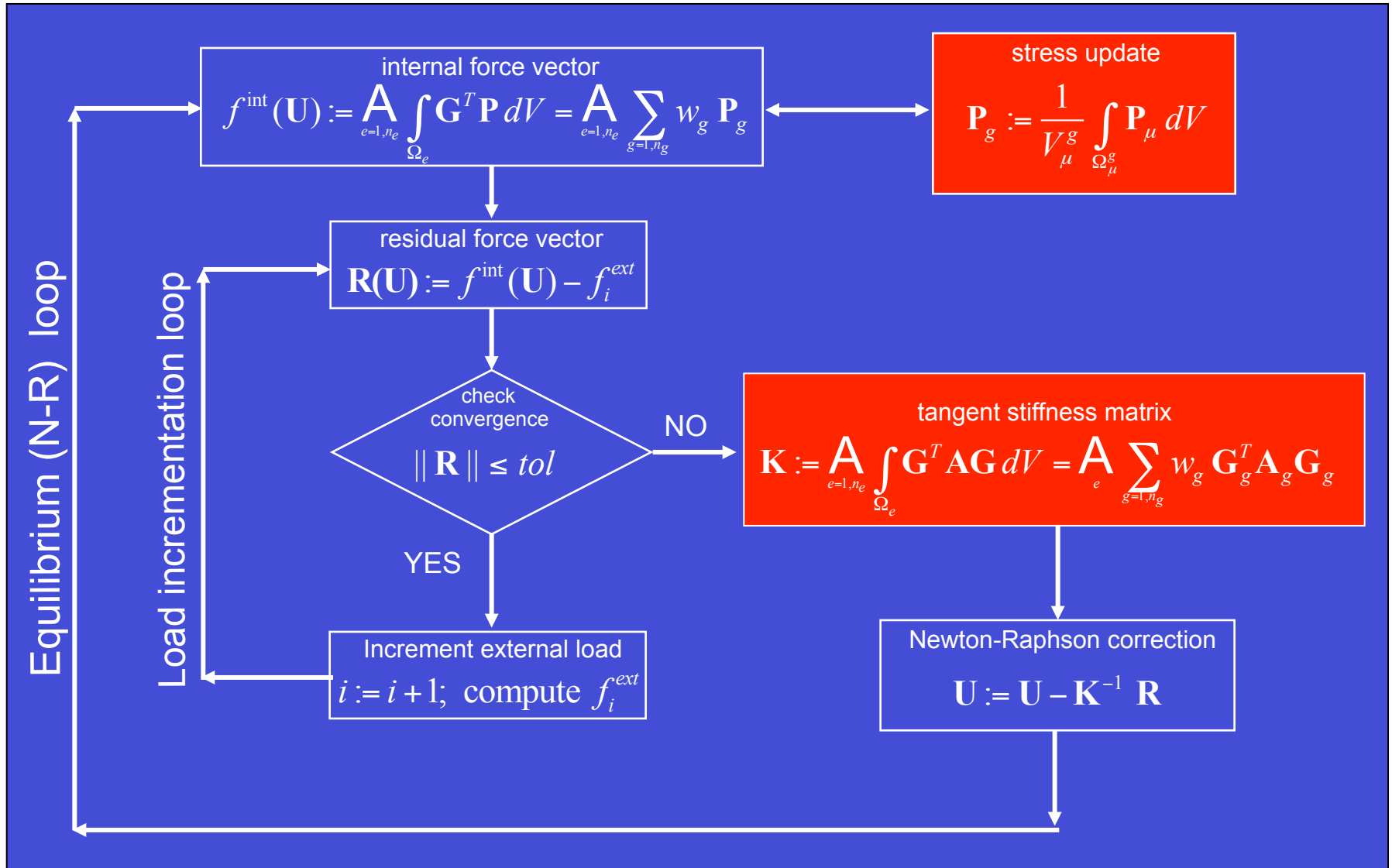
Linearised system

$$\left\{ \begin{array}{l} \left[\mathbf{F}_i \right]^{(k-1)} \\ \left[\mathbf{F}_f \right] \\ \left[\mathbf{F}_d \right] \end{array} + \begin{array}{l} \left[\mathbf{k}_{ii} \quad \mathbf{k}_{if} \quad \mathbf{k}_{id} \right]^{(k-1)} \\ \left[\mathbf{k}_{fi} \quad \mathbf{k}_{ff} \quad \mathbf{k}_{fd} \right] \\ \left[\mathbf{k}_{di} \quad \mathbf{k}_{df} \quad \mathbf{k}_{dd} \right] \end{array} \begin{array}{l} \left[\delta \tilde{\mathbf{u}}_i \right]^{(k)} \\ \left[\delta \tilde{\mathbf{u}}_f \right] \\ \left[\mathbf{R} \delta \tilde{\mathbf{u}}_f \right] \end{array} \right\} \cdot \begin{array}{l} \left[\eta_i \right] \\ \left[\eta_f \right] \\ \left[\mathbf{R} \eta_f \right] \end{array} = 0 \quad \forall \eta_i, \eta_f$$

Final format

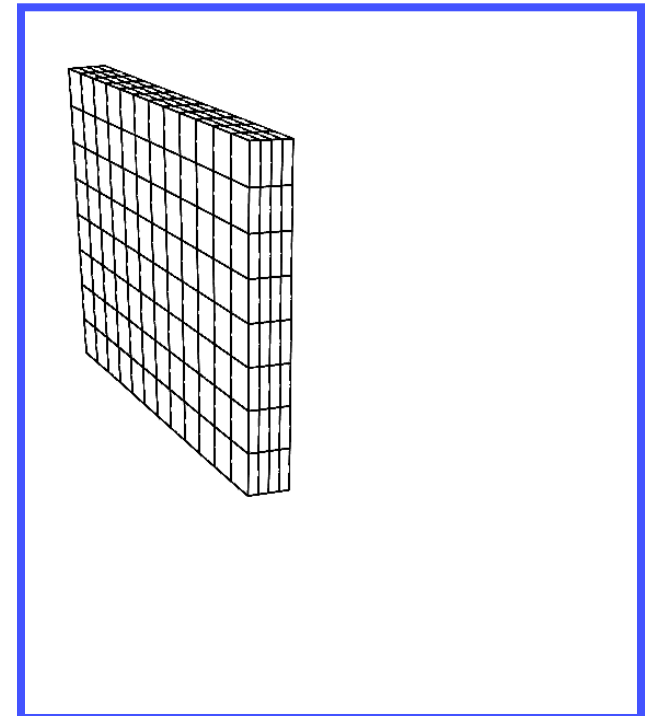
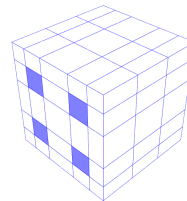
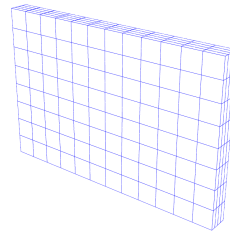
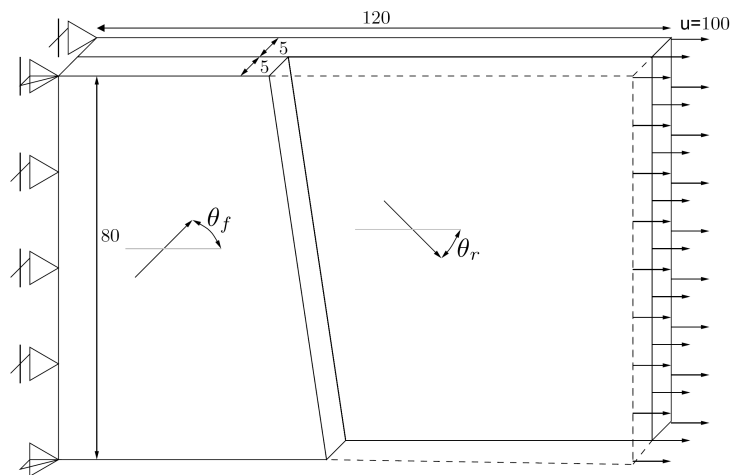
$$\begin{array}{l} \left[\begin{array}{cc} \mathbf{k}_{ii} & \mathbf{k}_{if} + \mathbf{k}_{id} \mathbf{R} \\ \mathbf{k}_{fi} + \mathbf{R}^T \mathbf{k}_{di} & \mathbf{k}_{ff} + \mathbf{k}_{fd} \mathbf{R} + \mathbf{R}^T \mathbf{k}_{df} + \mathbf{R}^T \mathbf{k}_{dd} \mathbf{R} \end{array} \right]^{(k-1)} \begin{array}{l} \left[\delta \tilde{\mathbf{u}}_i \right]^{(k)} \\ \left[\delta \tilde{\mathbf{u}}_f \right] \end{array} = - \begin{array}{l} \left[\mathbf{F}_i \right]^{(k-1)} \\ \left[\mathbf{F}_f + \mathbf{R}^T \mathbf{F}_d \right] \end{array} \end{array}$$

Fully coupled multiscale analysis



Fully coupled FE analysis. Example

Hyperelastic composite. Two-ply laminate



Multiscale constitutive theory

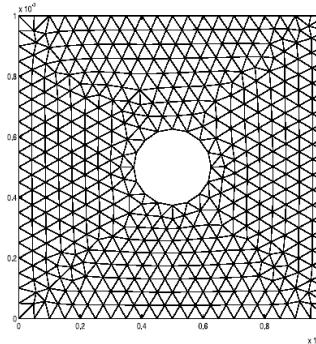
Typical applications

- Coupled multiscale FE analysis (FE^2)
- **Calibration of phenomenological (macroscopic) models**
- Devising new macroscopic models
- Understanding microscopic mechanisms and their impact on macroscopic behaviour
- Design/optimisation of microstructures

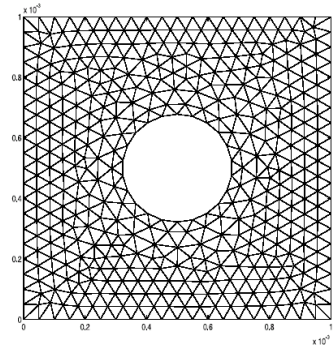
Linear elastic microstructures

No need for coupled analysis as the homogenised constitutive tensor defines completely the macroscopic behaviour !

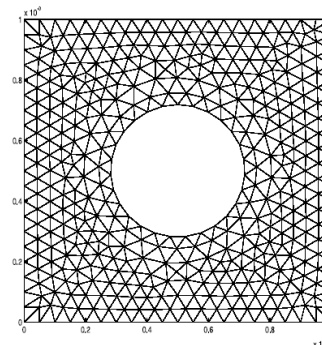
Example:
Linear elastic porous material



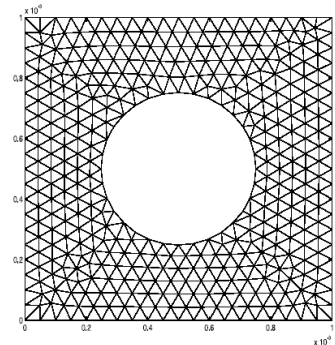
Type 1
5% VVF



Type 2
10% VVF



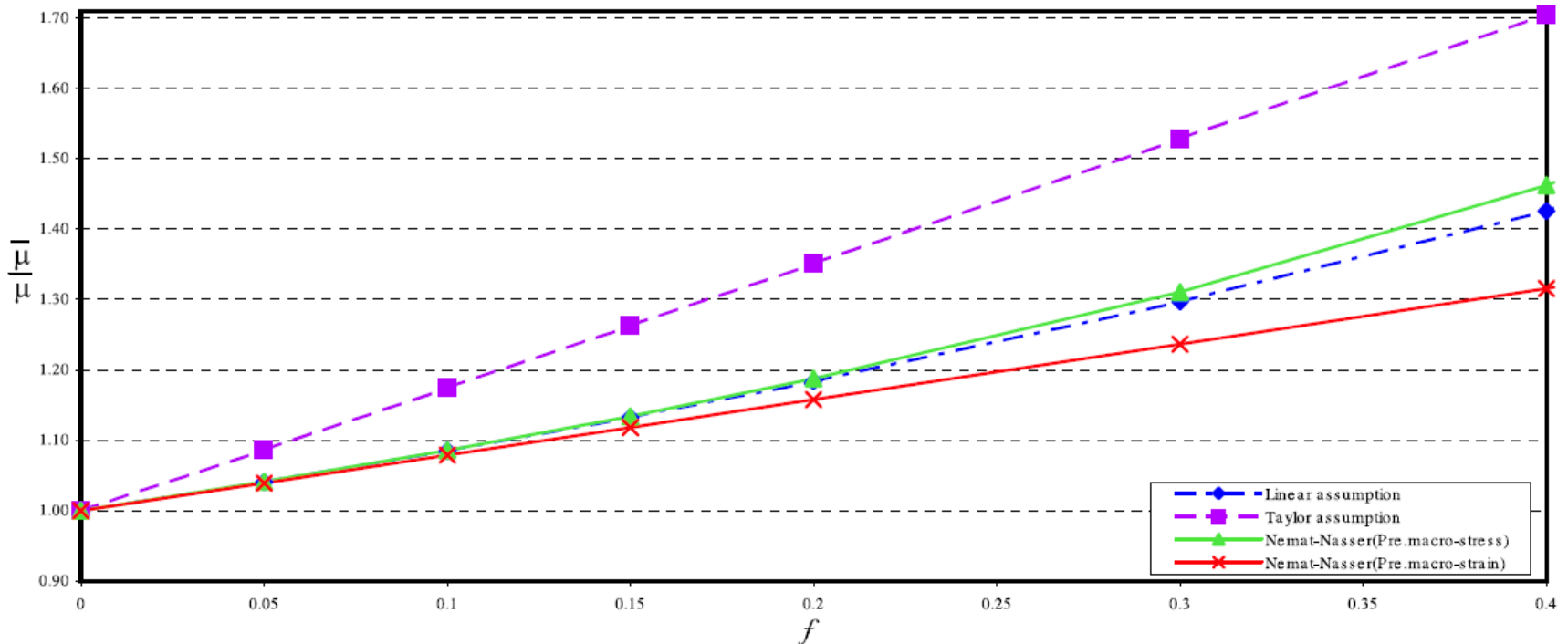
Type 3
15% VVF



Type 4
20% VVF

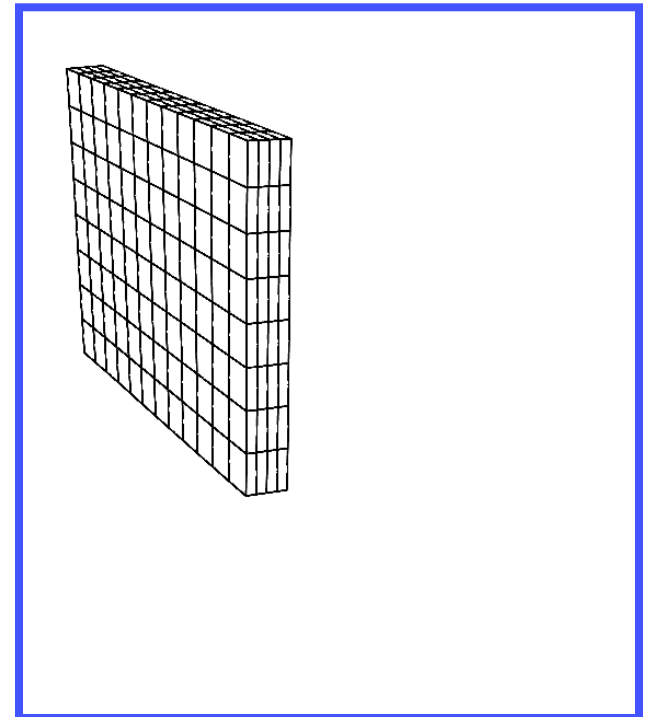
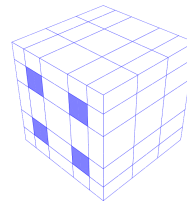
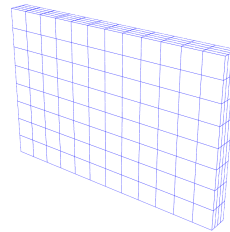
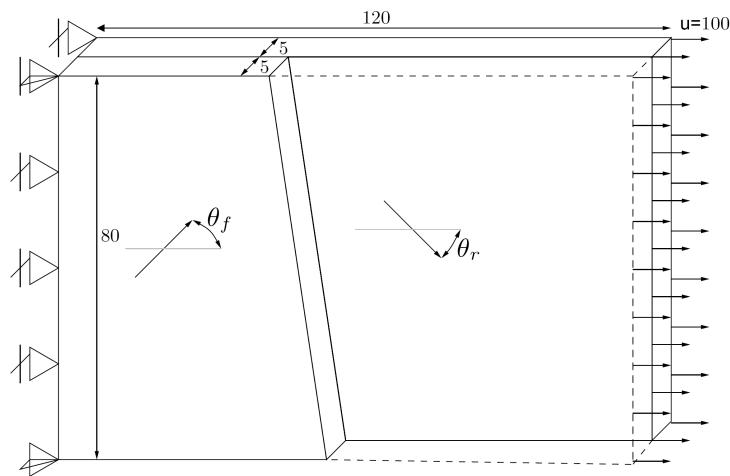
Example: Linear elastic porous material

Shear modulus as a function of void volume fraction
(need only compute elasticity tensor)



...back to a previous example

Hyperelastic composite. Two-ply laminate



- Single-Scale Transversely Isotropic Continuum Model:

$$\Psi_{iso} = \frac{\mu}{2}(I_1 - 3) - \mu \ln J + \frac{\lambda}{2}(J - 1)^2$$

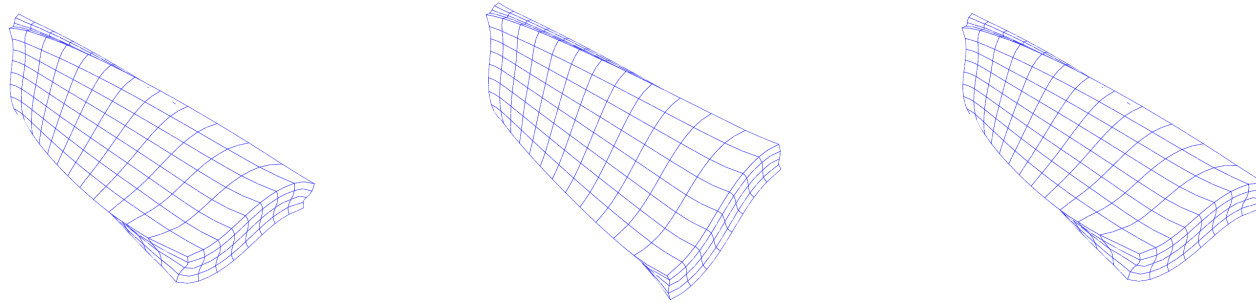
$$\Psi_{trn} = [\alpha + \beta \ln J + \gamma(I_4 - 1)](I_4 - 1) - \frac{\alpha}{2}(I_5 - 1).$$

Bonet J., Burton A.J., A simple orthotropic, transversely isotropic hyperelastic constitutive equation for large strain computations, *Comput. Methods Appl. Mech. Engrg.*, **162** (1998) 151-164.

- Multi-Scale Model with Isotropic Neo-Hookean Matrix:

$$\Psi_{mat} = \frac{\mu}{2}(I_1 - 3) - \mu \ln J + \frac{\lambda}{2}(J - 1)^2$$

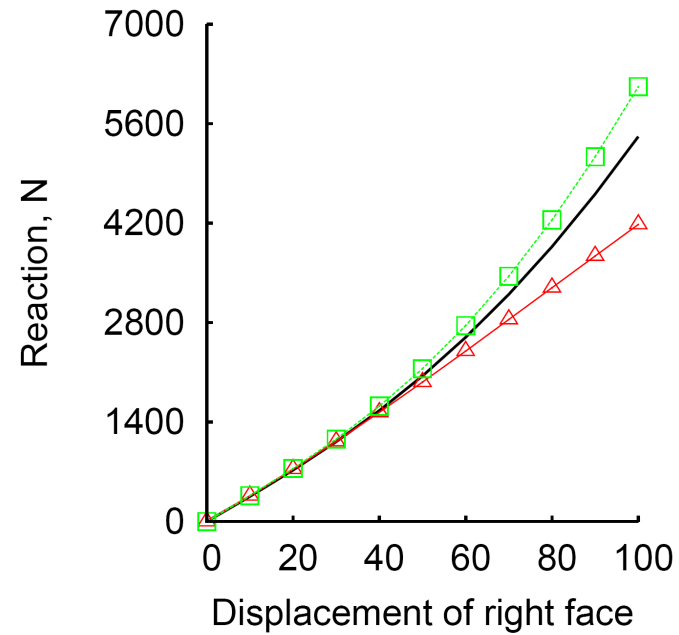
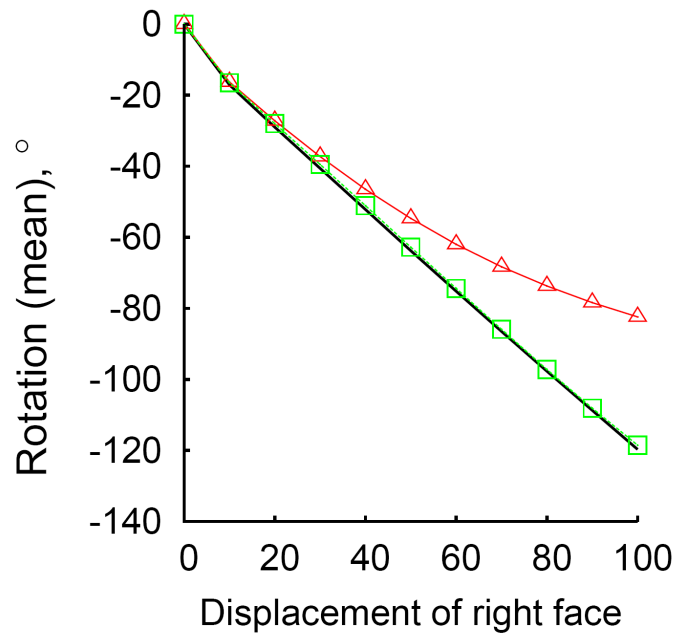
- Isotropic **Neo-Hookean Fiber**: $\Psi_{neo} = \Psi_{mat}$
- Isotropic **Ogden Fiber**: $\Psi_{ogd} = \sum_{n=1}^N \frac{\mu_n}{\alpha_n} (\lambda_1^{\alpha_n} + \lambda_2^{\alpha_n} + \lambda_3^{\alpha_n} - 3)$
 N is a positive integer, $\lambda_{i(i=1,2,3)}$ are the principal stretches and μ_n and α_n are material constants such that $\mu_n \alpha_n > 0$, $n = 1, 2, \dots, N$



Single-Scale Model

RVE (Neo-Hookean Fibre)

RVE (Ogden Fibre)



Multiscale constitutive theory

Typical applications

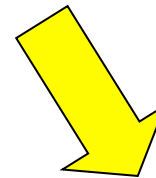
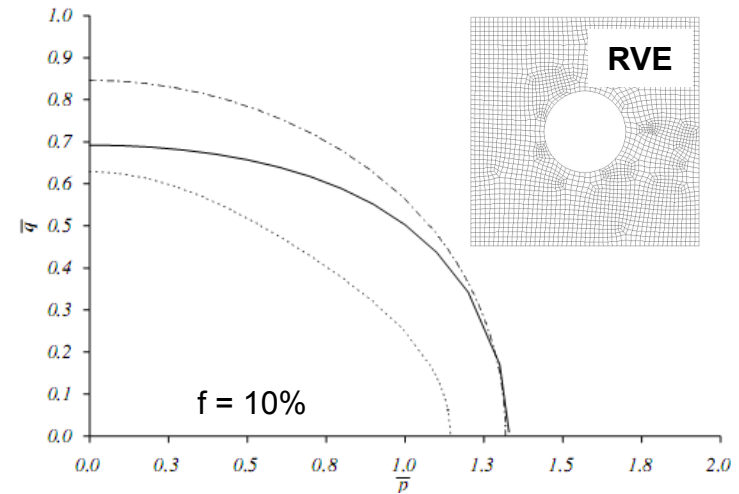
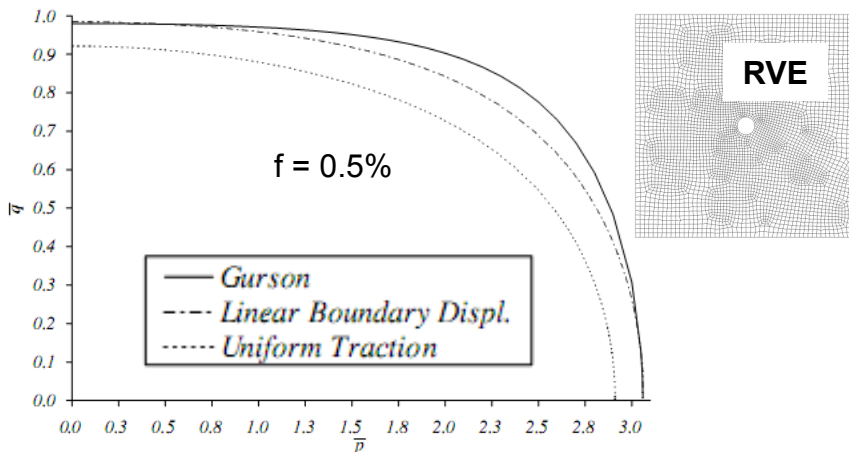
- Coupled multiscale FE analysis (FE^2)
- Calibration of phenomenological (macroscopic) models
- **Devising new macroscopic models**
- Understanding microscopic mechanisms and their impact on macroscopic behaviour
- Design/optimisation of microstructures

Application. Devising new models

Porous plasticity

$$\bar{\boldsymbol{\varepsilon}} = \alpha \begin{bmatrix} \frac{1}{\sqrt{2}} & 0 \\ 0 & \frac{1}{\sqrt{2}} \end{bmatrix} + \sqrt{1 - \alpha^2} \begin{bmatrix} 0 & \frac{1}{\sqrt{2}} \\ \frac{1}{\sqrt{2}} & 0 \end{bmatrix}$$

$\alpha \in [0, 1]$



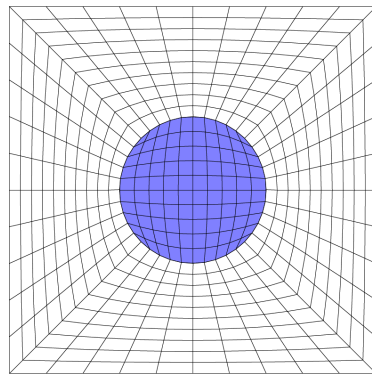
Macroscopic yield function

$$\bar{\Phi} = q - C_1 \left[1 - C_2 \sin^2 \left(\frac{\pi p}{2P_m} \right) \right] \left\{ \frac{1}{C_{eq}} \left[1 + f^2 - 2fC_3 \cosh \left(\frac{\sqrt{3}C_4 p}{\sigma_Y} \right) \right] \right\}^{\frac{1}{2}} \sigma_Y$$

Application. *Devising new models*

Plasticity with phase debonding

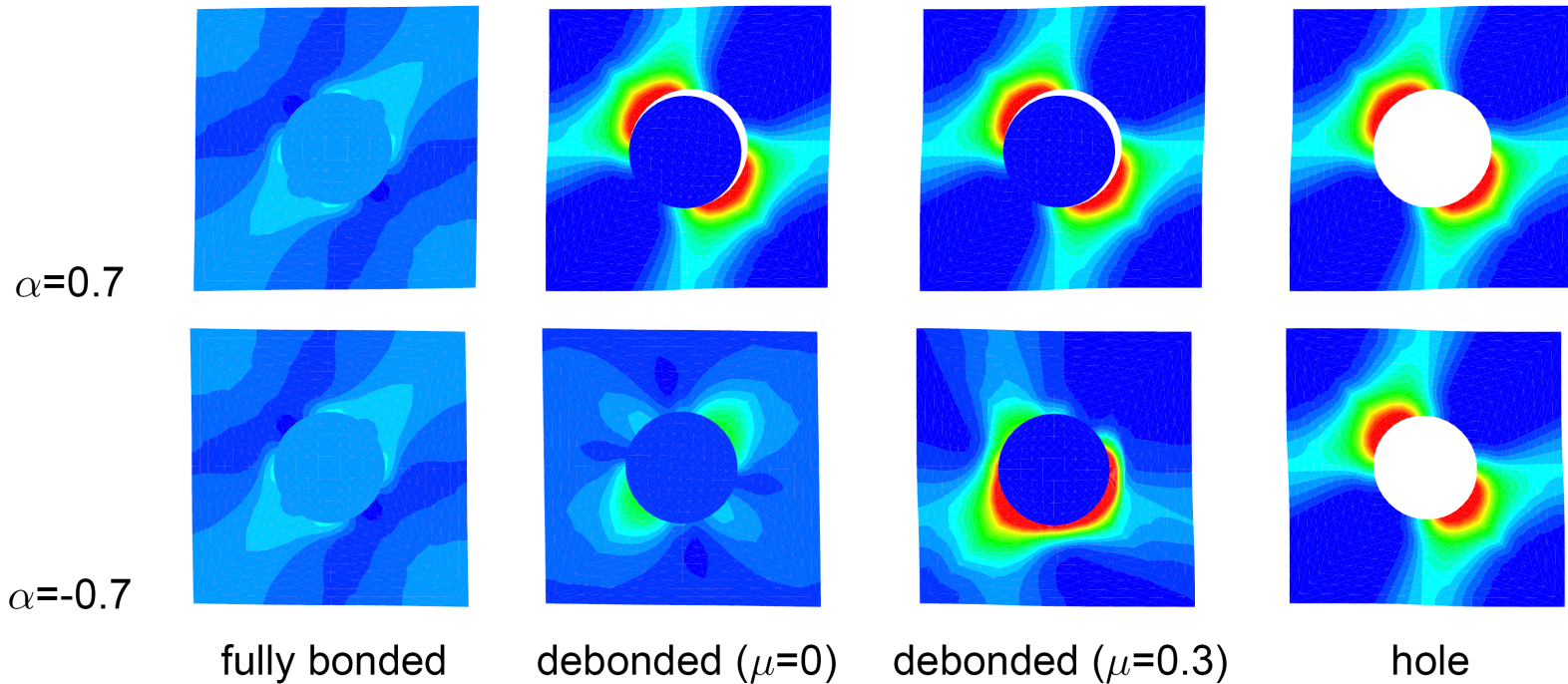
$$\bar{\boldsymbol{\varepsilon}} = \alpha \begin{bmatrix} \frac{1}{\sqrt{2}} & 0 \\ 0 & \frac{1}{\sqrt{2}} \end{bmatrix} + \sqrt{1 - \alpha^2} \begin{bmatrix} 0 & \frac{1}{\sqrt{2}} \\ \frac{1}{\sqrt{2}} & 0 \end{bmatrix}, \quad \alpha = -1.0, -0.9, \dots, 0, \dots, 1.0$$



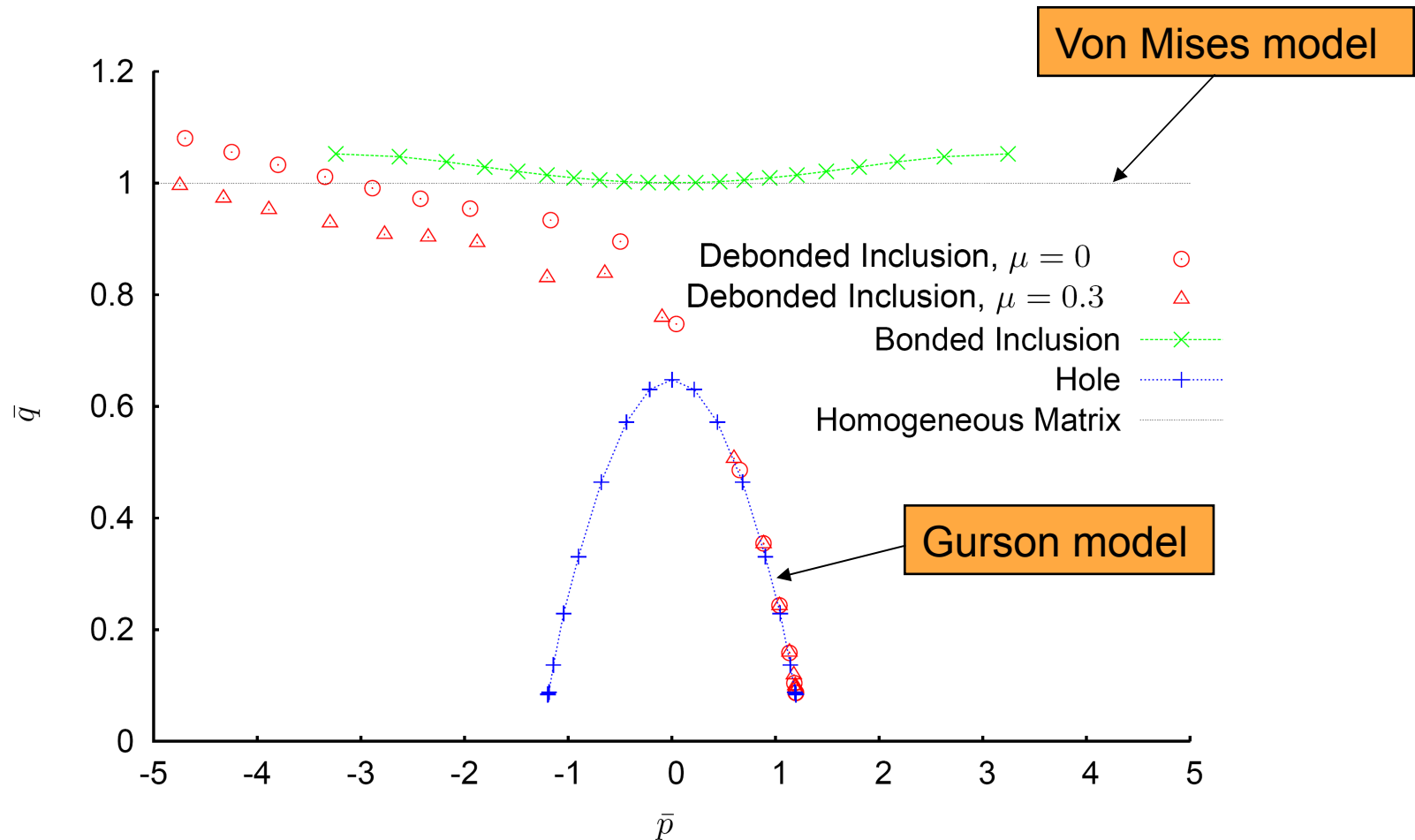
- ideally plastic matrix
- rigid inclusion
- contact with ($\mu=0.3$) and without ($\mu=0$) friction

$$\bar{\boldsymbol{\sigma}}^{coll} \Rightarrow \left\{ \begin{array}{l} p^{coll} = \frac{1}{3} \sum_{i=1}^3 \bar{\sigma}_{ii}^{coll} \\ q^{coll} = \sqrt{\frac{3}{2} (\bar{\boldsymbol{\sigma}}^{coll} - p\mathbf{I}) : (\bar{\boldsymbol{\sigma}}^{coll} - p\mathbf{I})} \end{array} \right\} \Rightarrow \left\{ \begin{array}{l} \bar{p} = \frac{p^{coll}}{\sigma_Y} \\ \bar{q} = \frac{q^{coll}}{\sigma_Y} \end{array} \right\}$$

Plasticity with phase debonding



Plasticity with phase debonding. *Homogenised yield surfaces*

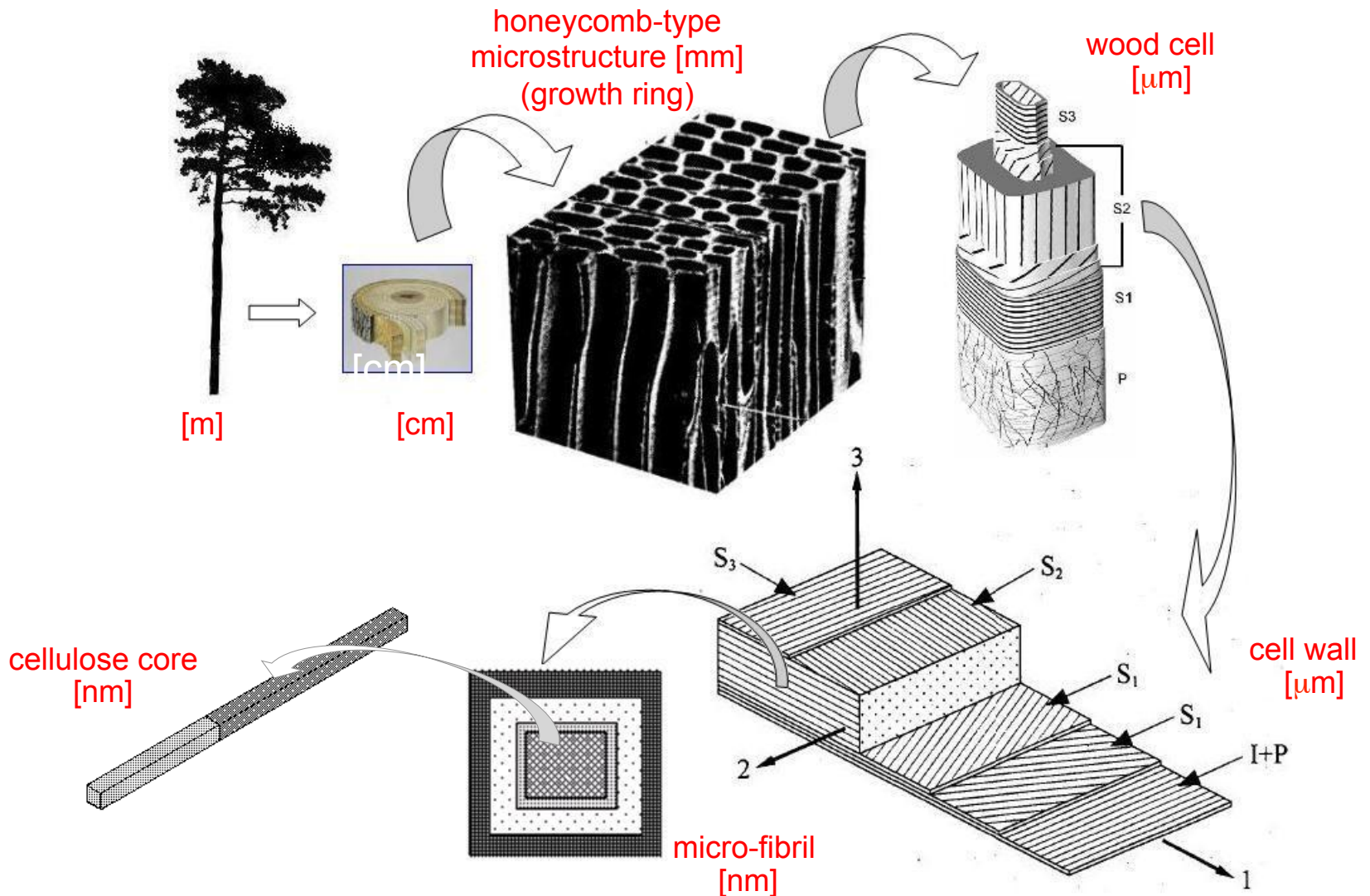


Multiscale constitutive theory

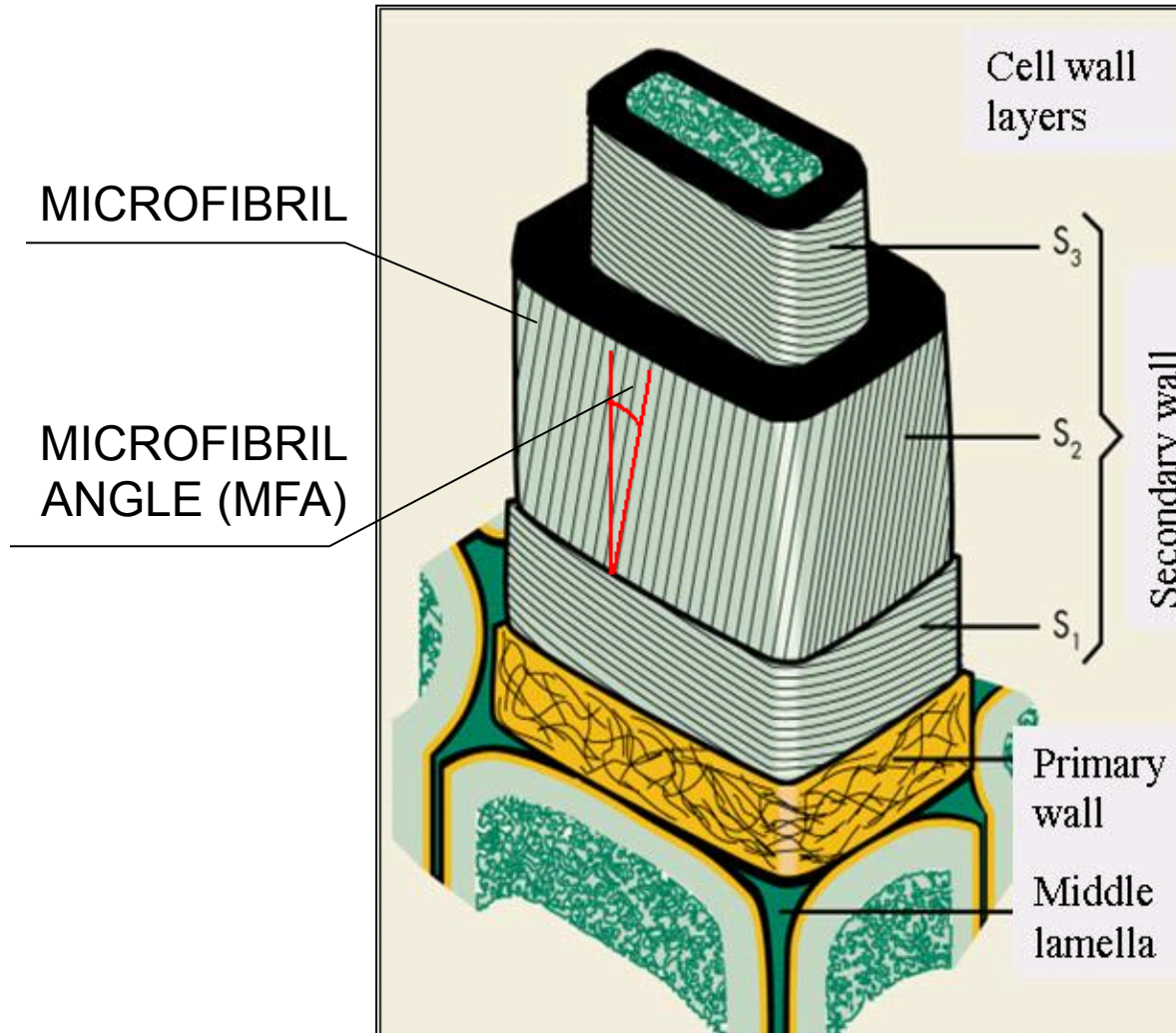
Typical applications

- Coupled multiscale FE analysis (FE^2)
- Calibration of phenomenological (macroscopic) models
- Devising new macroscopic models
- **Understanding microscopic mechanisms and their impact on macroscopic behaviour**
- Design/optimisation of microstructures

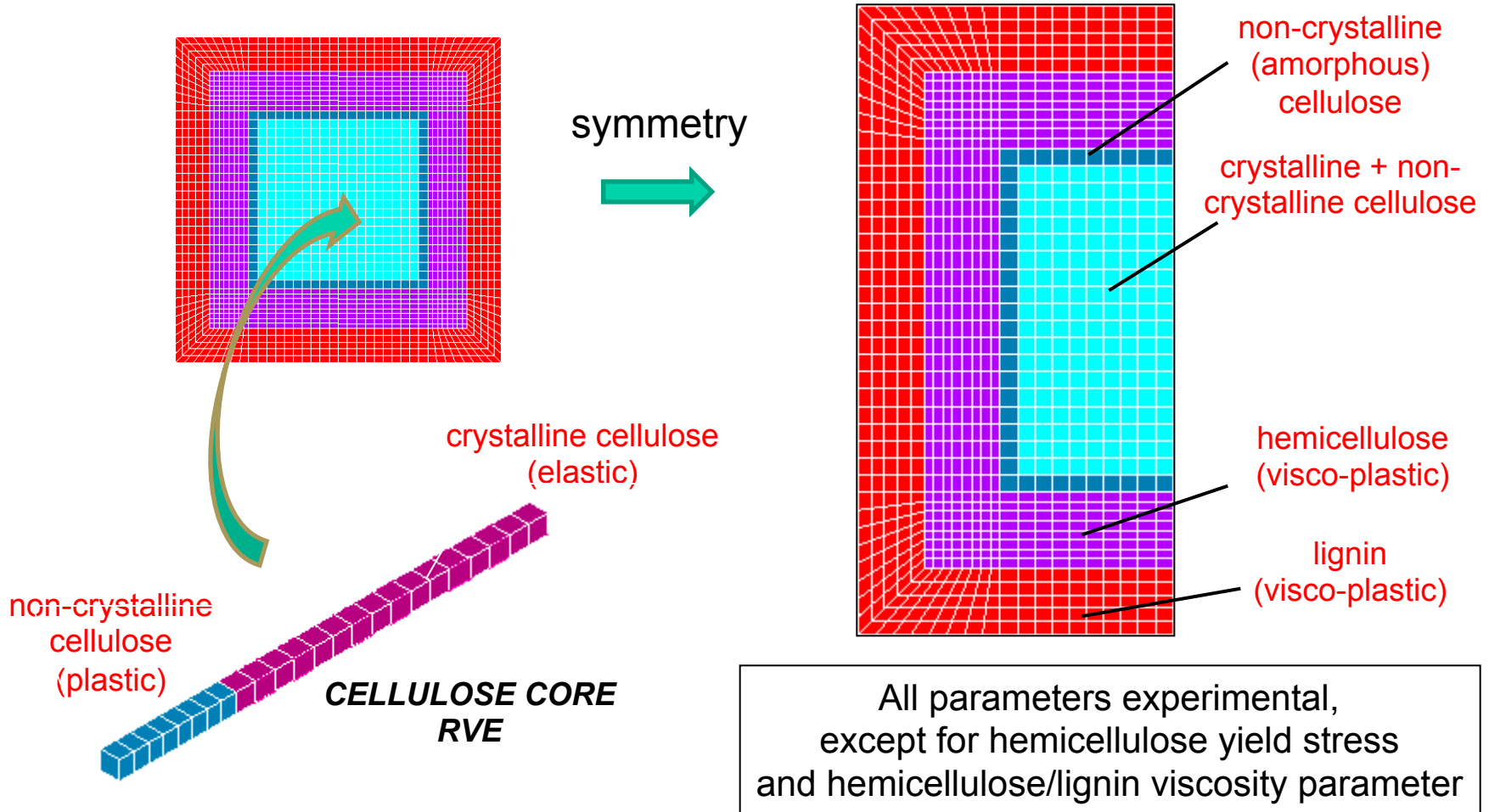
Application. Understanding dissipative behaviour Wood cell-wall



Application. Understanding dissipative behaviour Wood cell-wall

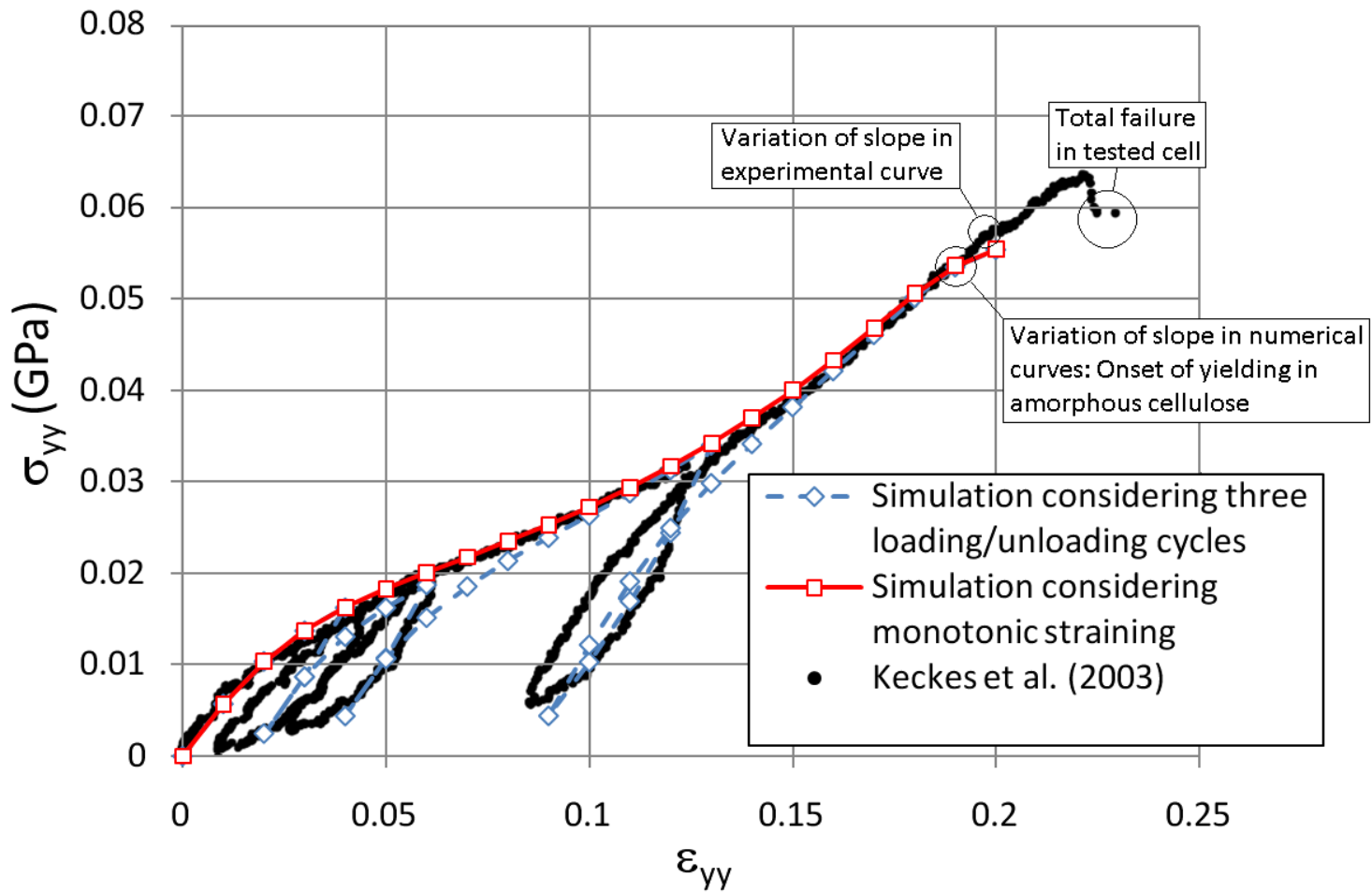


2-scale 3-D microfibril (cell-wall level) RVE



Application. Understanding dissipative behaviour Wood cell-wall

(Saavedra Flores, de Souza Neto, Comput. Mat. Sci., 2011)



Multiscale constitutive theory

Typical applications

- Coupled multiscale FE analysis (FE^2)
- Calibration of phenomenological (macroscopic) models
- Devising new macroscopic models
- Understanding microscopic mechanisms and their impact on macroscopic behaviour
- **Design/optimisation of microstructures**

Application

Microstructural design/optimisation

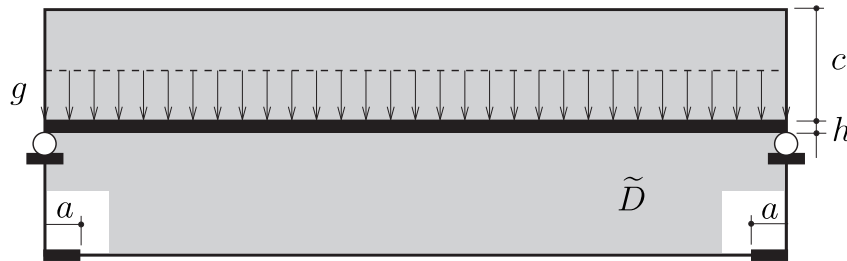
The idea

- To develop a **topological derivative-based** algorithm for the optimisation/design of elastic microstructures

The reason

- Success of the approach in the optimisation of load-bearing structures – **simple algorithms**
- Current methods of topological optimisation rely heavily on artificial algorithmic parameters and ad-hoc post-processing techniques

Example of topological derivative-based design optimisation



Initial bridge design guess



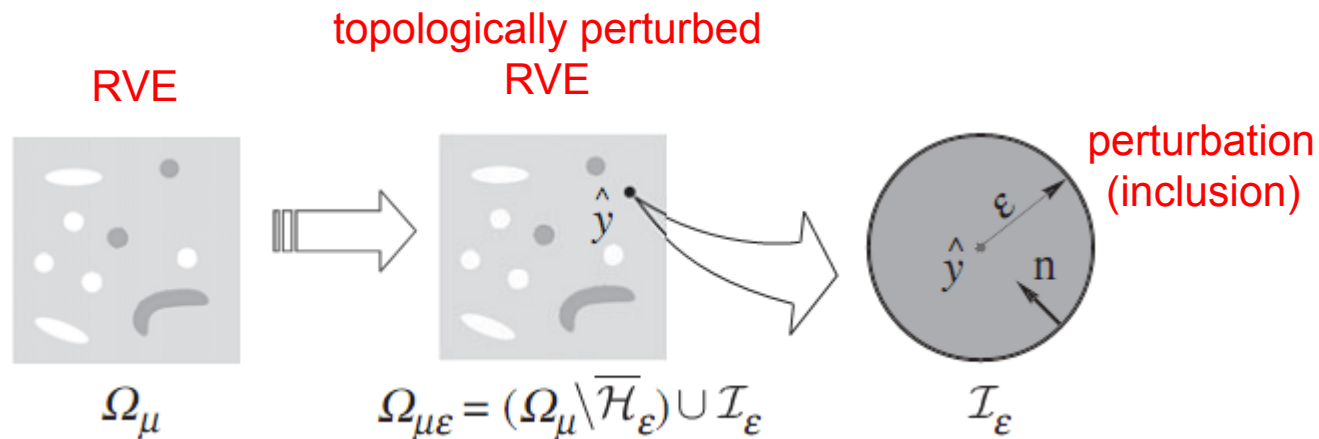
Optimum design – von Mises stress constraint



Optimum design – Drucker-Prager stress constraint

Topological optimisation/design of elastic microstructures

The **topological derivative** (Sokolowski & Zochowski, 1999) here will be associated with the following topological perturbation of the microscopic domain:



topological asymptotic expansion of a functional

$$\psi(\Omega_{\mu\epsilon}(\hat{\mathbf{y}})) = \psi(\Omega_\mu) + f(\epsilon) D_T \psi(\hat{\mathbf{y}}) + o(f(\epsilon))$$

where $f(\epsilon) \rightarrow 0$, when $\epsilon \rightarrow 0^+$.

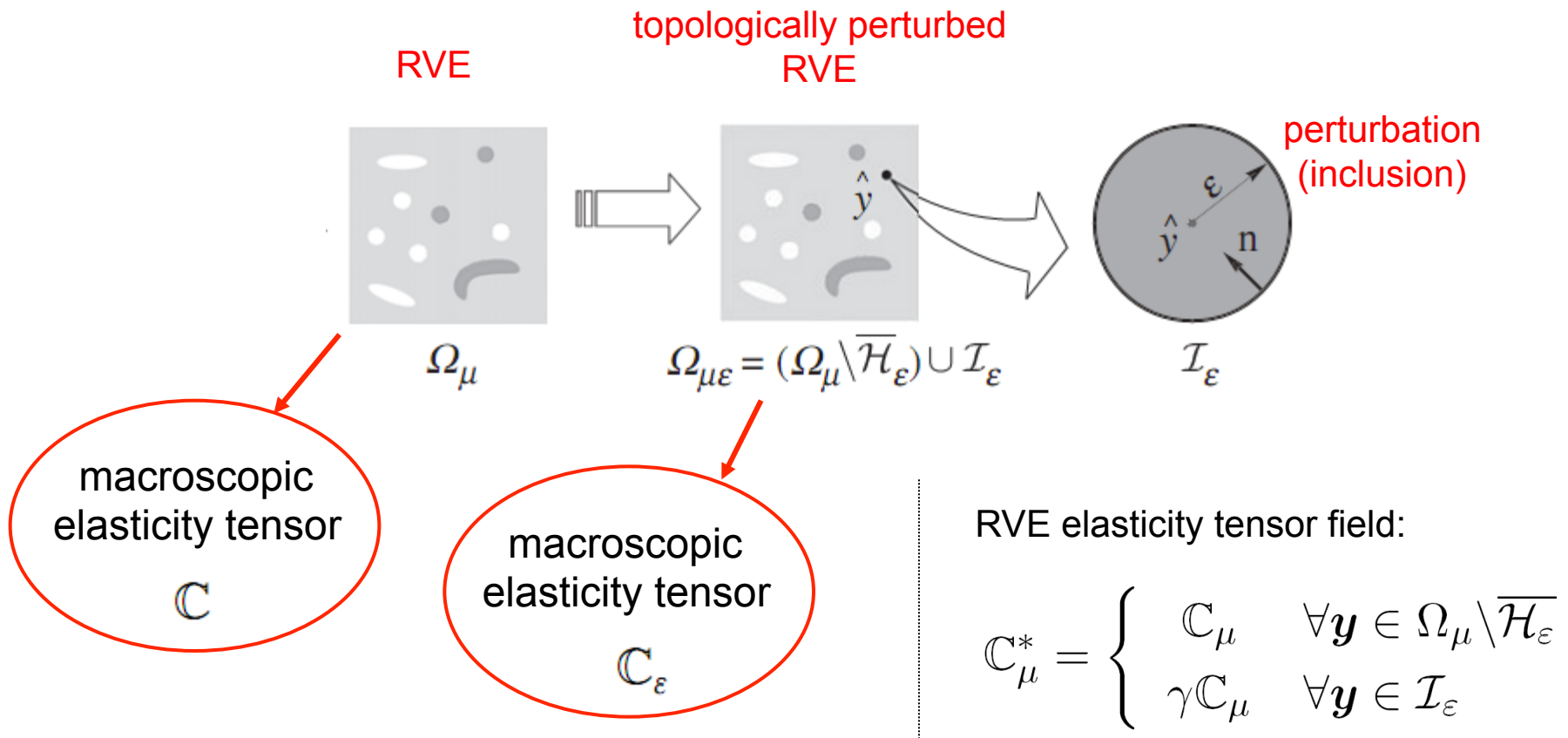
topological derivative

$$D_T \psi = \lim_{\epsilon \rightarrow 0} \frac{\psi(\Omega_{\mu\epsilon}) - \psi(\Omega_\mu)}{f(\epsilon)}$$

$$f(\epsilon) = |B_\epsilon|$$

Topological optimisation/design of elastic microstructures

Problem definition



Topological optimisation/design of elastic microstructures

The macroscopic elasticity tensor

$$\mathbb{C} = \bar{\mathbb{C}} + \tilde{\mathbb{C}}$$

where $\bar{\mathbb{C}}$ is the Taylor (volume average) elasticity tensor and

$$\tilde{\mathbb{C}} = \left[\frac{1}{V_\mu} \int_{\Omega_\mu} (\tilde{\mathbb{T}}_{\mu kl})_{ij} \right] (\mathbf{e}_i \otimes \mathbf{e}_j \otimes \mathbf{e}_k \otimes \mathbf{e}_l) \quad \tilde{\mathbb{T}}_{\mu ij} = \mathbb{C}_\mu \nabla^s \tilde{\mathbf{u}}_{\mu ij}$$

$$\int_{\Omega_\mu} \mathbb{C}_\mu \nabla^s \tilde{\mathbf{u}}_{\mu ij} \cdot \nabla^s \boldsymbol{\eta} = - \int_{\Omega_\mu} \mathbb{C}_\mu (\mathbf{e}_i \otimes \mathbf{e}_j) \cdot \nabla^s \boldsymbol{\eta} \quad \forall \boldsymbol{\eta} \in \mathcal{V}_\mu$$

Topological optimisation/design of elastic microstructures

Topological asymptotic expansion of the macro elasticity tensor
 (Giusti, Novotny & de Souza Neto. *Proc. R. Soc. A*, 2010)

$$\psi(\varepsilon) := \mathcal{J}_{\Omega_{\mu\varepsilon}}(\mathbf{u}_{\mu\varepsilon}) = \int_{\Omega_{\mu\varepsilon}} \mathbf{T}_{\mu\varepsilon} \cdot \nabla^S \mathbf{u}_{\mu\varepsilon}$$

$$D_T \psi = \lim_{\varepsilon \rightarrow 0} \frac{1}{f'(\varepsilon)} \frac{d}{d\varepsilon} \mathcal{J}_{\Omega_{\mu\varepsilon}}(\mathbf{u}_{\mu\varepsilon})$$

$$\frac{d}{d\varepsilon} \mathcal{J}_{\Omega_{\mu\varepsilon}}(\mathbf{u}_{\mu\varepsilon}) = \int_{\Omega_{\mu\varepsilon}} \boldsymbol{\Sigma}_{\mu\varepsilon} \cdot \nabla \mathbf{v} \quad \boldsymbol{\Sigma}_{\mu\varepsilon} = (\mathbf{T}_{\mu\varepsilon} \cdot \mathbf{E}_{\mu\varepsilon}) \mathbf{I} - 2(\nabla \tilde{\mathbf{u}}_{\mu\varepsilon})^T \mathbf{T}_{\mu\varepsilon}$$

$$\mathbf{T}^\varepsilon \cdot \mathbf{E} = \mathbf{T} \cdot \mathbf{E} - v(\varepsilon) \mathbb{H} \mathbf{T}_\mu \cdot \mathbf{T}_\mu + o(v(\varepsilon))$$

$$v(\varepsilon) := \pi \varepsilon^2 / V_\mu$$

Topological optimisation/design of elastic microstructures

Topological asymptotic expansion of \mathbb{C}

$$\mathbb{C}_\varepsilon = \mathbb{C} - v(\varepsilon)\mathbb{D}_{T\mu} + o(v(\varepsilon))$$

$$\mathbb{D}_{T\mu} = \mathbb{H} \tilde{\mathbf{T}}_{\mu_{ij}} \cdot \tilde{\mathbf{T}}_{\mu_{kl}} (\mathbf{e}_i \otimes \mathbf{e}_j \otimes \mathbf{e}_k \otimes \mathbf{e}_l)$$

topological
derivative of
 \mathbb{C}



$$\mathbb{H} := \frac{1}{E} \left(\frac{1 - \gamma}{1 + \alpha\gamma} \right) \left[4\mathbb{I} + \frac{\gamma(\alpha - 2\beta) - 1}{1 + \beta\gamma} (\mathbf{I} \otimes \mathbf{I}) \right] \quad \alpha := \frac{3 - \nu}{1 + \nu} \quad \beta := \frac{1 + \nu}{1 - \nu}$$

Limits:

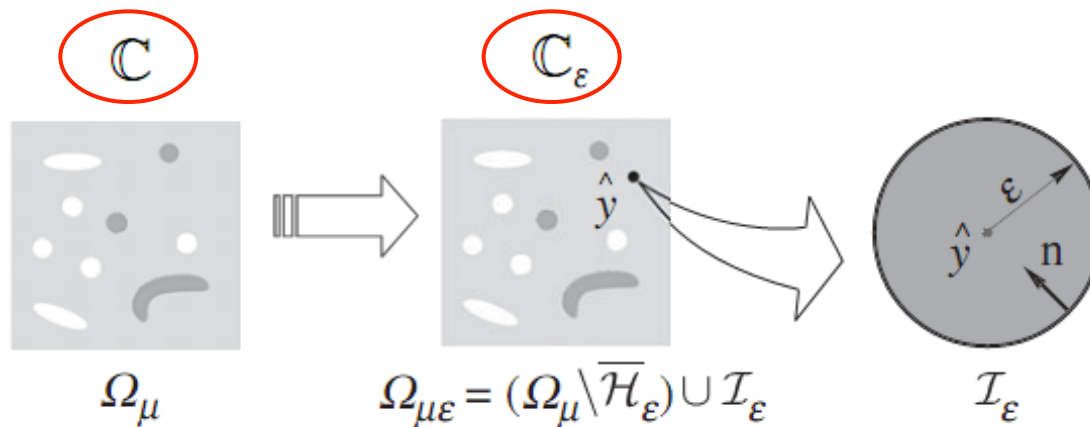
$\gamma \rightarrow 0$ (insertion of void)

$\gamma \rightarrow \infty$ (rigid inclusion)

$$\mathbb{H} = \frac{1}{E} [4\mathbb{I} - (\mathbf{I} \otimes \mathbf{I})]$$

$$\mathbb{H} = -\frac{1}{E\alpha} \left[4\mathbb{I} + \frac{\alpha - 2\beta}{\beta} (\mathbf{I} \otimes \mathbf{I}) \right]$$

Topological optimisation/design of elastic microstructures



The field $\mathbb{D}_{T\mu}$ at each point \hat{y} of the RVE represents the derivative of \mathbb{C} with respect to the volume fraction of inclusion inserted at that point.

Topological optimisation/design of elastic microstructures

The optimisation problem (bi-material micro-structure)

$$\text{Minimize } J(\Omega_\mu^1) = h(\mathbb{C}) + r_i \left[\frac{|\Omega_\mu^1|}{V_\mu} - \frac{|\Omega_\mu^{1*}|}{V_\mu} \right]^2$$

$$\Omega_\mu^1 \subset \Omega_\mu$$

Topological derivative-based optimisation algorithm

(Amstutz, Giusti, Novotny, de Souza Neto. IJNME, 2010)

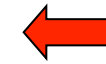
$$D_T J(y) = \langle Dh(\mathbb{C}), D_T \mathbb{C}(y) \rangle + 2r_i (V_\mu^1 - V_\mu^{1*})$$



topological derivative of cost function J

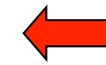
$$\Omega_\mu^1 = \{y \in \Omega_\mu, \psi(y) < 0\}$$

$$\Omega_\mu^2 = \{y \in \Omega_\mu, \psi(y) > 0\}$$



level-set domain representation

$$\exists \tau > 0 \quad \text{s.t.} \quad g = \tau \psi \quad g(y) = \begin{cases} -D_T J(\Omega_\mu^1)(y) & \text{if } y \in \Omega_\mu^1 \\ D_T J(\Omega_\mu^1)(y) & \text{if } y \in \Omega_\mu^2 \end{cases}$$



Sufficient optimality condition

$$D_T J(y) > 0 \quad \forall y \in \Omega_\mu$$

$$\psi_{n+1} = \frac{1}{\sin \theta_n} \left[\sin((1 - \kappa_n)\theta_n) \psi_n + \sin(\kappa_n \theta_n) \frac{g_n}{\|g_n\|_{L^2}} \right]$$

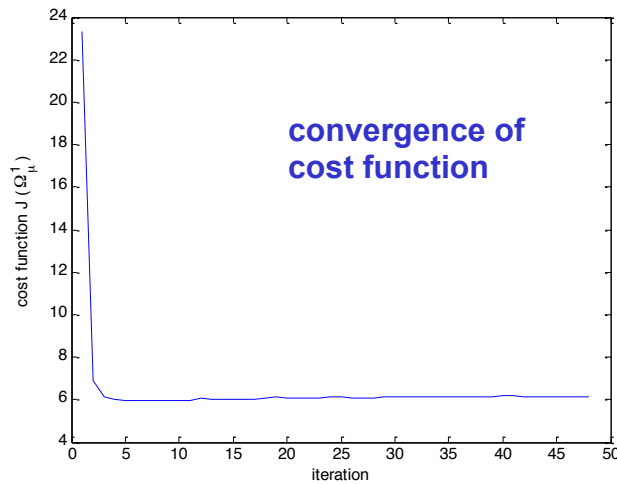
$$\psi_0 \in \mathcal{S}$$



fixed point iteration

EXAMPLE 1 – Maximisation of Bulk modulus with specified volume fraction

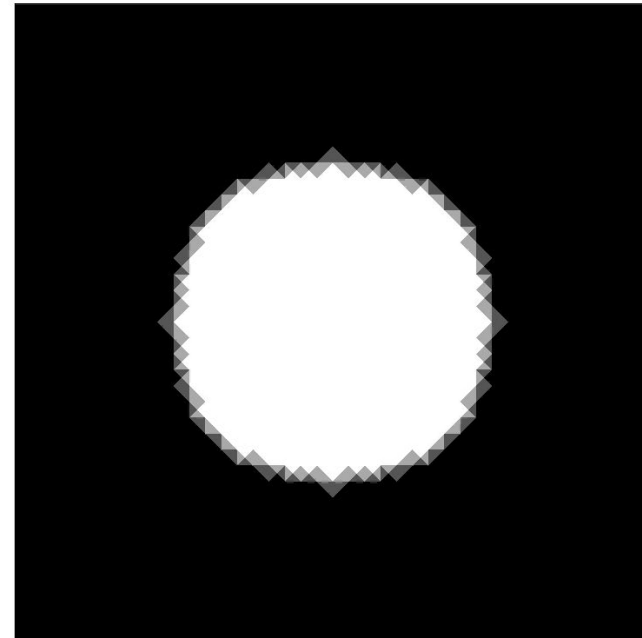
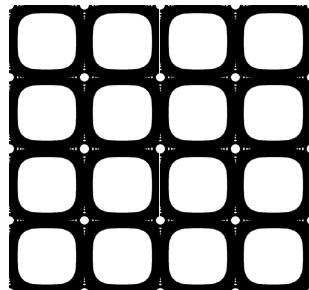
Target volume fraction of phase 1 = 0.44



$$h(\mathbb{C}) = (\mathbb{C}^{-1})_{1111} + 2(\mathbb{C}^{-1})_{1122} + (\mathbb{C}^{-1})_{2222}$$

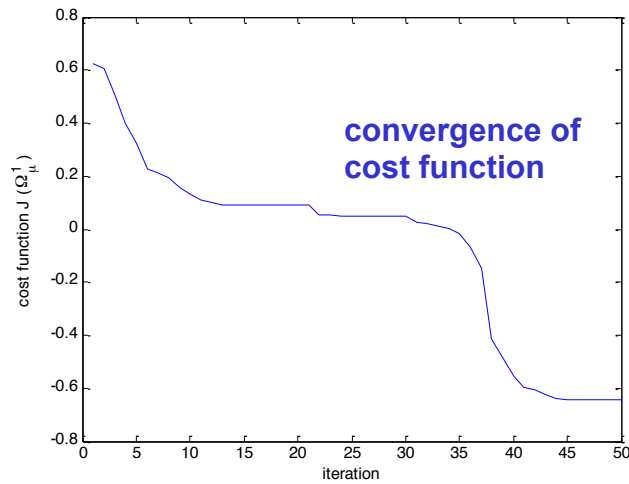
designed
microstructure

$K = 0.1640$
 $V_f = 0.4444$



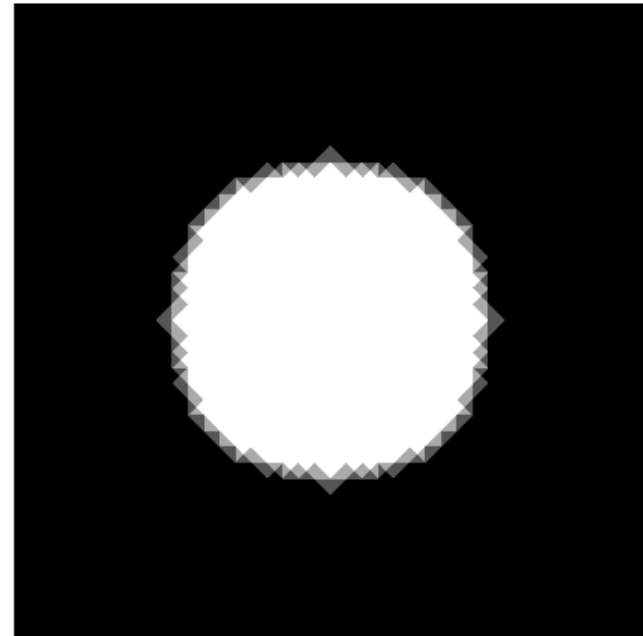
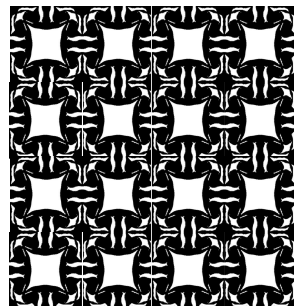
EXAMPLE 2 – Minimisation of Poisson ratio with specified volume fraction

Target volume fraction of phase 1 = 0.66

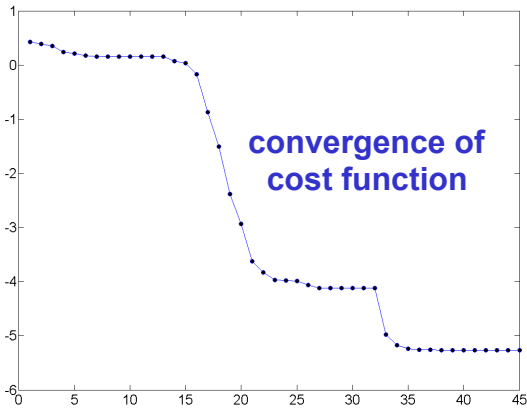


designed microstructure

Poiss = -0.322
Vf = 0.655

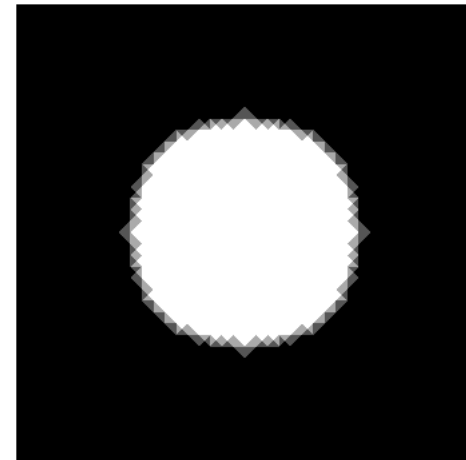
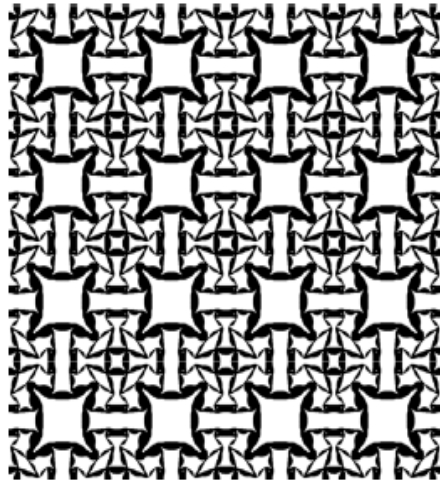


EXAMPLE 3 – Poisson ratio minimisation



$$h(\mathbb{C}) = -(\mathbb{C}^{-1})_{1122}$$

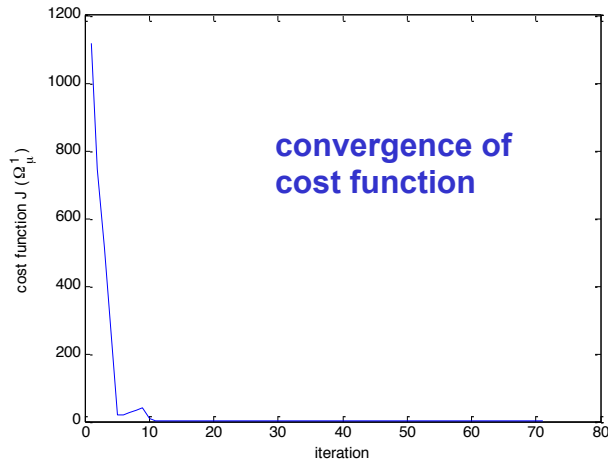
optimised microstructure



EXAMPLE 4 – Microstructure *design* to specified property

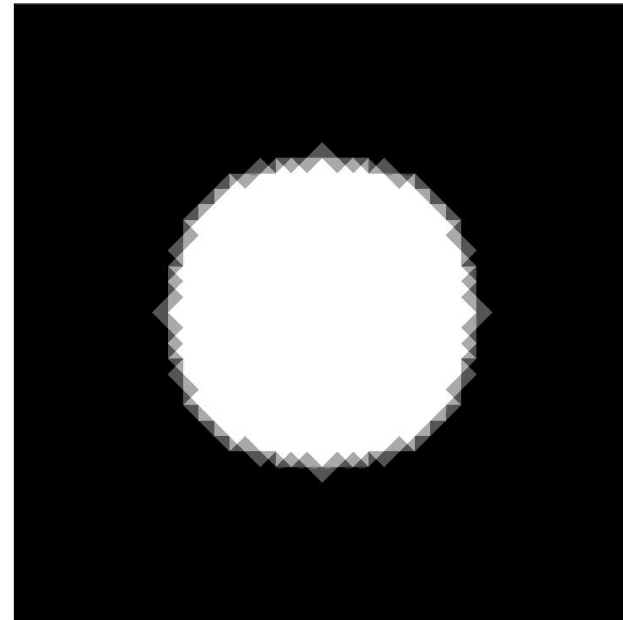
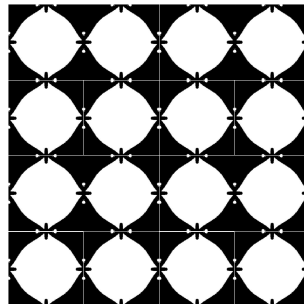
Target Bulk Modulus = 0.1

Target volume fraction of phase 1 = 0.44

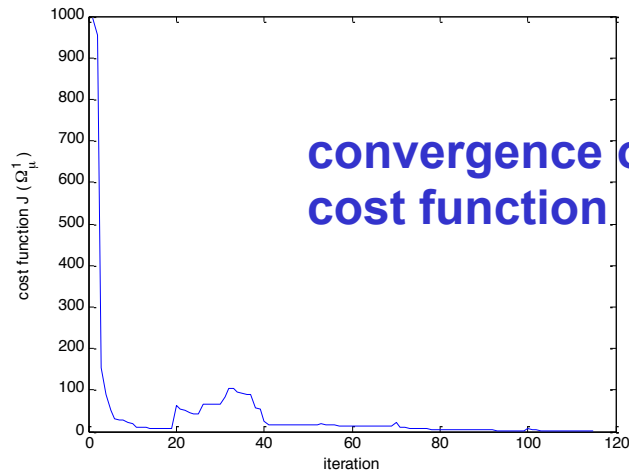


designed
microstructure

$K = 0.1003$
 $V_f = 0.4401$

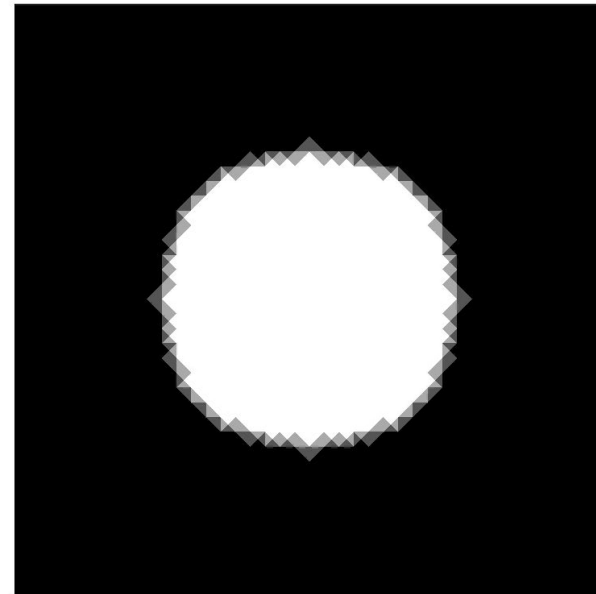
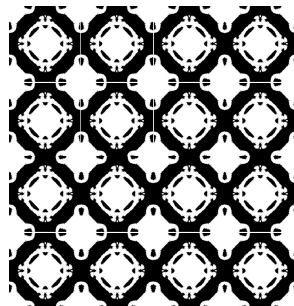


EXAMPLE 5 – Microstructure *design* to specified property
Target in-plane Poisson ratio = 0.8
Target volume fraction of phase 1 = 0.48



**designed
microstructure**

Poiss = 0.7899
Vf = 0.4803



Multiscale modelling

Current challenges and ongoing work

- **Multiscale modelling/analysis:**
 - Alloys (phenomena such as grain boundary sliding, etc)
 - Hydrogen embrittlement/hydrogen diffusion
- **Microstructural design/optimisation:**
 - Manufacturing constraints
 - Bio-inspired materials
 - Biocompatible materials
 - Stress intensity factor constraints (?)
 - Metamaterials (?)